



LAWRENCE
LIVERMORE
NATIONAL
LABORATORY

Methods of Calculation of Resistance to Polarization (Corrosion Rate) Using ASTM G 59

L. L. Wong, K. J. King, S. I. Martin, R. B. Rebak

February 6, 2006

Disclaimer

This document was prepared as an account of work sponsored by an agency of the United States Government. Neither the United States Government nor the University of California nor any of their employees, makes any warranty, express or implied, or assumes any legal liability or responsibility for the accuracy, completeness, or usefulness of any information, apparatus, product, or process disclosed, or represents that its use would not infringe privately owned rights. Reference herein to any specific commercial product, process, or service by trade name, trademark, manufacturer, or otherwise, does not necessarily constitute or imply its endorsement, recommendation, or favoring by the United States Government or the University of California. The views and opinions of authors expressed herein do not necessarily state or reflect those of the United States Government or the University of California, and shall not be used for advertising or product endorsement purposes.

This work was performed under the auspices of the U.S. Department of Energy by University of California, Lawrence Livermore National Laboratory under Contract W-7405-Eng-48.

not conventional (Figure 1b). The polarization resistance obtained for the specific example given in Figure 1b is $R_p = 2.27 \times 10^6 \text{ Ohm.cm}^2$, the same than for the older software version in Figure 1a.

However, if in *Echem Analyst 1.3* the operator chooses to plot Potential (Y) vs. Current Density (X), i.e. in the standard convention used in corrosion, the software does not reverse the axes before fitting as the *Launcher Version 3.10* used to do. That is, with *Echem Analyst 1.3* a fit is made, but this is not correct since the sum of least squares fit is not performed for the dependent variable (Current Density). The equation in the software is still correct, but the independent variable (Potential) is actually being “fitted” by the software (Figure 2). The polarization resistance (R_p) thus obtained is lower than from Figures 1a and 1b (correct way). Also, Figure 2 shows that the fit is poor and this is especially obvious when the data appears “noisy” and/or nonlinear.

Figure 3 shows an example of another way of calculating polarization resistance (corrosion rate). The *Echem Analyst 1.3* software allows the manual placing of a line on the gathered data on a E(Y) vs. I(X) curve. The slope of this line is R_p .

PURPOSE OF THIS PAPER

This paper was prepared to document ways of calculating corrosion rates from electrochemical measurements according to ASTM G 59. This process was triggered by the change in software by Gamry. The new software used in the standard way (potential in Y axis) was puzzling the operators since the fit of the data was poor (see for example Figure 2). Therefore many operators resorted to using a manual fit of the potential (Y) vs. current (X) data, which is an “option” in *Echem Analyst 1.3* (Figure 3). The manual fitting resulted in a value of R_p that represented the data better than according to *Echem Analyst 1.3* (e.g. Figure 2).

Therefore, in this paper three methods used to report and compare values of R_p and corrosion rate from polarization resistance data. All three analysis are generated by using Gamry *Echem Analyst 1.3* software.

Method 1: Using the Echem Analyst Polarization Resistance Calculation routine embedded in the Echem Analyst software with the test Applied Voltage plotted on the Y-Axis and the test resultant Current Density plotted on the X-axis. The value of the CR reported by this method is for informative purposes only just to document a recent changes in the Gamry software. This is the least valid of the three methods since it fits the slope against the rules of linear regression analysis, which requires the plotting the E in the X axis as the independent variable.

Method 2: Using the Echem Analyst Polarization Resistance Calculation routine embedded in the Echem Analyst software with the test resultant Current Density plotted on the Y-Axis and the test Applied Voltage plotted on the X-axis. This is proper method mathematically.

Method 3: Using the Echem Analyst slope calculation routine which allows the software user to draw an interactive on-screen slope line in the on-screen plot of the polarization resistance data. The Echem analyst software then calculates the slope of this manually inserted line. Using this slope value the software user can then use an Excel spreadsheet and appropriate equations to calculate a corrosion rate based on the slope.

EXPERIMENTAL RESULTS

The experimental results are presented either as polarization resistance (R_p) in $\text{Ohm}\cdot\text{cm}^2$ or as corrosion rates (CR) in $\mu\text{m}/\text{year}$. These two quantities are inversely proportional to each other, that is, the higher the R_p the lower the CR. For Alloy 22 (N06022), the following equation can be used

$$CR\left(\frac{\mu\text{m}}{\text{year}}\right) = 2.28 \times 10^5 \frac{1}{R_p\left(\Omega \cdot \text{cm}^2\right)}$$

The proportionality constant was calculated assuming the equivalent weight of Alloy 22 to be 23.28 g, the density 8.69 g/cm^3 , and the Faraday constant 96,485 C/mol. For Alloy 22, an R_p value of 1 $\text{M}\Omega\cdot\text{cm}^2$ yields a corrosion rate of 0.228 $\mu\text{m}/\text{year}$.

Testing of Alloy 22 in MIC Experiments

Three welded discs of Alloy 22 were exposed to an electrolyte solution of 10 X J-13 water plus glucose nutrient at ambient temperature in three different vessels (V10, V11 and V12). The solution was inoculated with Yucca Mountain type microorganisms (Non-Sterile conditions). Sue Martin calculated the Resistance to Polarization (R_p) using Echem Analyst with current in the Y axis and potential in the X axis (Method 2) as well as using a manual fit (E in Y axis and current in the X axis) as in Method 3. The R_p values are plotted in Figure 4 as a function of a sequence number. The sequence number increases with the immersion time in the vessels. However, the time interval is not the same between sequence numbers. There are two or three R_p values for each vessel for each sequence number. Figure 4 shows that the R_p is approximately the same using both Methods 2 and 3. Taking an overall average of the R_p values for each method for all the sequence numbers in Figure 4, the average R_p values are 17.81 for Method 2 and 18.06 for Method 3. These are practically the same. The standard deviation was 25.95 for Method 2 and 17.51 for Method 3. That is, doing the R_p slope manually results in less error than using the Gamry Echem Analyst software.

Long Term Immersion of Alloy 22 Bars

This section shows results of testing from Gary Hust, John Estill, Marshall Stuart and Ken King and painstakingly analyzed and organized by Ken King. Figure 5 shows the corrosion rate of a MA Alloy 22 specimen (DEA2843) as a function of immersion time in 0.1 M oxalic acid solution at 30°C. Results were analyzed using Methods 1, 2 and 3. For each immersion time, there were three values of corrosion rates corresponding to three sequential Runs. The corrosion rate was approximately constant in time and between 0.15 $\mu\text{m}/\text{year}$ and 0.3 $\mu\text{m}/\text{year}$. Table 1 shows the average corrosion rate for the specimen in the tested time

interval according to each method of evaluation. The average corrosion rate was approximately the same at 0.2 $\mu\text{m}/\text{year}$ independently of the method used for calculation. The lowest standard deviation (SD) corresponded to Method 3 (Manual Fitting) and the largest to Method 1 (E in Y axis and current in X axis).

Table 1: Corrosion Rate of Alloy 22 (DEA2843) in 0.1 M Oxalic Acid at 30°C Cell 11 in Bench Top Experiments for Long Term E_{corr} Evaluation.

Method	Ave Corr Rate ($\mu\text{m}/\text{year}$)	Standard Deviation
1	0.222	0.054
2	0.209	0.044
3	0.218	0.023

Table 2 shows the average corrosion rate using the three methods of the MA Alloy 22 specimen DEA3087, which was immersed for long time in 1 M CaCl_2 + 1 M $\text{Ca}(\text{NO}_3)_2$ solution at 90°C. The average corrosion rate is for a total of three measurements at each testing time. The standard deviation (SD) values are also reported. Figure 6 shows a representation of the corrosion rates only for Methods 2 and 3. The value of corrosion rates using Method 1 was not included in Figure 6 since it had a large standard deviation at the highest time, therefore overshadowing the rest of the data in the figure. Method 3 generated the lowest corrosion rates; however, Figure 6 shows that the values were comparable to the ones generated using Method 2. The tendency of a decrease in the corrosion rate as the time increased was the same for Methods 2 and 3. Table 2 shows that the largest standard deviation corresponded to Method 1 and the lowest to Method 3 (Manual Fit).

Table 2: Corrosion Rate of Alloy 22 (DEA3087) in 1 M CaCl_2 + 1 M $\text{Ca}(\text{NO}_3)_2$ at 90°C Cell 13 in Bench Top Experiments for Long Term E_{corr} Evaluation.

Date	Immersion Time (Days)	Corrosion Rate ($\mu\text{m}/\text{year}$) \pm SD Method 1	Corrosion Rate ($\mu\text{m}/\text{year}$) \pm SD Method 2	Corrosion Rate ($\mu\text{m}/\text{year}$) \pm SD Method 3
31Jul03	457	0.511 \pm 0.496	0.124 \pm 0.086	0.075 \pm 0.014
15Sep03	503	0.143 \pm 0.049	0.090 \pm 0.033	0.052 \pm 0.030
28Oct03	546	-0.080 \pm 1.100	0.074 \pm 0.093	0.065 \pm 0.045

Table 3 shows the average corrosion rate using the three methods of the MA Alloy 22 specimen DEA2805, which was immersed for long time in 5 M CaCl_2 + 0.5 M $\text{Ca}(\text{NO}_3)_2$ solution at 90°C. The average corrosion rate is for a total of three measurements at each testing time. The standard deviation (SD) values are also reported. Figure 7 shows a representation of the corrosion rates only for Methods 2 and 3. The value of corrosion rates using Method 1 was not included in Figure 7 since it had a large standard deviation and negative corrosion rate at the first testing time, therefore overshadowing the rest of the data in the figure. Negative corrosion rate are of no physical significance and a result of noisy electrochemical measurements. For the testing times between 467 days and 698 days, the corrosion rate between all three methods were similar (Table 3), independently of the

immersion time and approximately 0.15 $\mu\text{m}/\text{year}$. Method 3 generated the lowest standard deviation (SD) of the three methods (Figure 7 and Table 3).

Table 3: Corrosion Rate of Alloy 22 (DEA2805) in 0.5 M CaCl_2 + 0.5 M $\text{Ca}(\text{NO}_3)_2$ at 90°C Cell 15 in Bench Top Experiments for Long Term E_{corr} Evaluation.

Date	Immersion Time (Days)	Corrosion Rate ($\mu\text{m}/\text{year}$) \pm SD Method 1	Corrosion Rate ($\mu\text{m}/\text{year}$) \pm SD Method 2	Corrosion Rate ($\mu\text{m}/\text{year}$) \pm SD Method 3
30Jul03	427	-3.40 \pm 7.013	0.082 \pm 0.085	0.169 \pm 0.016
08Sep03	467	0.234 \pm 0.008	0.160 \pm 0.043	0.272 \pm 0.070
27Oct03	516	0.253 \pm 0.785	0.121 \pm 0.106	0.116 \pm 0.018
26Apr04	698	0.318 \pm 0.129	0.145 \pm 0.127	0.134 \pm 0.026

Figure 8 shows the calculation of the corrosion rates of Alloy 22 immersed in Simulated Acidified Water (SAW) without silicates in the solution (Cell 17 in the long term monitoring of E_{corr}). This solution was naturally aerated and maintained at 90°C. Figure 8 shows the corrosion rate data between the immersion times of 180 days and 402 days for three type of materials: (1) Mill Annealed (MA) bar (DEA2813), (2) As-Welded (ASW) bar (JE2042) and (3) Welded Plus Thermally Aged (WPA) bar (JE2014). The thermal aging of JE2014 was carried at 700°C for 173 h. All three methods show that the corrosion rate of Alloy 22 increased as the immersion time increased. No explanation is offered at this time for this phenomenon since it is beyond the purpose of this document. It is expected that for a passivating metal such as Alloy 22, the corrosion rate will decrease as the testing time increased. Figure 8 also shows that the corrosion rate of the MA material was the highest and the corrosion rate of the ASW material was the lowest. These results seem consistent and no explanation is offered at this time either. More importantly for this paper, Figure 8 shows that the corrosion rate of each type of Alloy 22 material was practically the same using either one of the three methods of calculation analyzed here. Method 1 yielded in general the highest corrosion rate but results from Methods 2 and 3 were basically identical. Considering all three materials for the four tested times, the lowest standard deviation corresponded to Method 3 and the highest for Method 1.

Figure 9 and Table 4 show the corrosion rate for three Alloy 22 specimens, MA DEA2816, ASW JE2045 and WPA JE2017. Table 4 also shows the standard deviation of three measurements of corrosion rate at each time for each specimen. The largest variation in the corrosion rate corresponded to values calculated using Method 1. This method also yielded the largest standard deviation (Table 4). Figure 10 shows the corrosion rate of Alloy 22 in 4 M NaCl at 90°C for ASW and WPA specimens. The lowest corrosion rate corresponded to the WPA specimen. Figure 10 also shows that the corrosion rates values calculated using Methods 2 and 3 were similar to each other for each specimen. Method 3 yielded the lowest standard deviation (Table 4 and Figure 10). Table 4 shows that Method 2 could produce negative corrosion rates in cases of noisy data.

Table 4: Corrosion Rate of Alloy 22 in 4 M NaCl at 90°C
Cell 18 in Bench Top Experiments for Long Term E_{corr} Evaluation.

Date	Immersion Time (Days)	Corrosion Rate (µm/year) ± SD Method 1	Corrosion Rate (µm/year) ± SD Method 2	Corrosion Rate (µm/year) ± SD Method 3
MA DEA2816				
23Jul03	124	2.387 ± 1.407	0.422 ± 0.248	0.315 ± 0.009
26Aug03	158	0.884 ± 0.086	0.351 ± 0.175	0.293 ± 0.041
23Oct03	216	-2.995 ± 8.995	0.026 ± 0.062	0.146 ± 0.015
12Feb04	328	2.979 ± 4.431	2.860 ± 4.388	2.611 ± 3.774
ASW JE2045				
23Jul03	124	0.0789 ± 0.011	0.062 ± 0.012	0.064 ± 0.004
26Aug03	158	1.708 ± 1.562	0.037 ± 0.008	0.049 ± 0.007
23Oct03	216	0.708 ± 0.595	0.178 ± 0.181	0.127 ± 0.029
12Feb04	328	1.294 ± 1.844	0.065 ± 0.037	0.094 ± 0.027
WPA JE2017				
23Jul03	124	12.895 ± 22.278	0.006 ± 0.004	0.010 ± 0.002
26Aug03	158	0.365 ± .0554	0.014 ± 0.009	0.010 ± 0.005
23Oct03	216	-1.496 ± 1.933	-0.014 ± 0.028	0.014 ± 0.004
12Feb04	328	0.586 ± 0.932	0.011 ± 0.007	0.020 ± 0.000

Corrosion Behavior of Alloy 22 MA discs in Aerated SAW at 90°C

The corrosion behavior of Alloy 22 discs in aerated SAW solution at 90°C was evaluated as a function of time for six specimens. Figure 11 shows the polarization resistance (Rp) using Method 2 for the six specimens as a function of the immersion time in the solution. There are two Rp values for each specimen for each testing time. In general, for the few first days of immersion, Rp increased as the time increased. However, there were two specimens (JE1429 and JE1431) for which the Rp showed the largest discrepancy. Figure 11 shows that using a single method of calculating the individual polarization resistances (Method 2) can yield a wide variety of results from test to test, i.e. varying from specimen to specimen at each testing time. Figure 12 and Table 5 show the average corrosion rates for the six specimens listed in Figure 11 for the first five days of immersion using all three methods. Table 5 also lists the standard deviation in the corrosion rate considering all six specimens at each immersion time. Method 1 yielded higher corrosion rates than Method 2, even though the trend is the same. The average corrosion rates values between Methods 2 and 3 are practically indistinguishable (Figure 12). The lowest SD corresponded to Method 3 (Table 5).

Table 5: Corrosion Rate of Alloy 22 in aerated SAW at 90°C
Average Corrosion Rate from Six Disc Specimens at each Immersion Time
Specimens: JE1430, JE1432, JE1435, JE1436, JE1431 and JE1429.

Immersion Time (Days)	Corrosion Rate ($\mu\text{m}/\text{year}$) \pm SD Method 1	Corrosion Rate ($\mu\text{m}/\text{year}$) \pm SD Method 2	Corrosion Rate ($\mu\text{m}/\text{year}$) \pm SD Method 3
1	1.236 \pm 0.298	0.962 \pm 0.445	0.527 \pm 0.081
2	0.708 \pm 0.448	0.177 \pm 0.102	0.222 \pm 0.067
3	0.399 \pm 0.124	0.193 \pm 0.103	0.170 \pm 0.094
4	0.452 \pm 0.591	0.141 \pm 0.125	0.143 \pm 0.111
5	0.417 \pm 0.254	0.112 \pm 0.120	0.087 \pm 0.013

Corrosion Behavior of Alloy 22 in 6 m NaCl and 6 m NaCl + 0.9 m KNO₃ at 100°C

Figures 13 and 14 show the individual polarization resistance values for Alloy 22 as a function of immersion time in aerated 6 m NaCl and 6 m NaCl + 0.9 m KNO₃ solutions at 100°C, respectively. Five specimens were tested in each solution. The total immersion time was four days. Figures 13 and 14 show that in general, as the immersion time increased to the second day the Rp increased. For both solutions the Rp was practically the same. Also, for each specimen at each testing time the value of Rp was practically the same using either Methods 1 or 2. At each testing time there was more variation in the corrosion rate between specimen and specimen than between method and method for each specimen (see for example data for Day 2 in either solution). Figures 15 and 16 show the average Rp values in the pure chloride and in the chloride plus nitrate solutions, respectively. The standard deviation of the data for the five specimens is also shown. Basically, the standard deviation is the same regardless of method used to calculate the Rp. Also, the average Rp is only slightly higher in the nitrate containing solution.

FINAL REMARKS

Three methods were presented here to illustrate the calculation of polarization resistance (corrosion rates) of Alloy 22 in a variety of environments. Method 1 is given for illustrative purposes only. Mathematically, the Method 1 for calculation of Rp is not correct. However, this document shows that the values of polarization resistance obtained using Method 1 are not too far off the values obtained using either Methods 2 or 3 (preferred). Method 1 often yields the highest corrosion rates and the largest standard deviations since the fitting of the data is not as accurate as using for example Method 2. Nevertheless, data presented here shows that there is usually more variation in the corrosion rates between specimen and specimen tested under identical environmental conditions than between Method 1 and Method 2 for a single specimen and condition.

Older values of corrosion rates that may have been calculated using Method 1 do not need to be revisited since they were never used in any modeling or lifetime prediction. Only trends

between temperature and temperature or mill annealed vs. thermally aged conditions were analyzed. Results from the current report shows that the trends in corrosion rate using Methods 1 and 2 were the same.

The most reproducible results are obtained with either Method 2 or Method 3. Mathematically Method 2 would be preferred to Method 3 since it can be easily reproduced by a second operator. Once the limits of potential are set, the software calculates the corrosion rate. It is worth noting here the surprising results obtained using Method 3. Even though Method 3 is operator dependent, the same ranking of Method 3 is found with respect to Method 2 (operator independent) was found using results from three different operators. Sue Martin did the manual calculations of the MIC results, Ken King did the fittings for the Long Term Bench top cells and Lana Wong did the calculations of the Alloy 22 discs. The results from all three operators show that the results from Method 3 were extremely close to the results from Method 2. Method 3 in all cases yielded the lowest standard deviation showing that the good eye of the operator generally surpasses the mathematical fitting of the I vs. E equation. The problem with Method 3 is that results cannot be precisely reproduced, even by the same operator. However, the error in Method 3 is still smaller than in Method 2.

CONCLUSIONS

- (1) Method 1 is not a proper way of calculating Polarization Resistance since the fitting of dependent to independent variable is reversed. However, the difference in the results from Method 2 (proper fitting) are generally overshadowed by differences between specimen and specimen in the same testing conditions.
- (2) Method 2 provides the proper mathematical fitting of I vs. E data. Results are mathematically reproducible by a second operator. High noise in the experimental results may still yield high standard deviations and, sometimes, negative corrosion rates.
- (3) Method 3 gives values of polarization resistance that are practically undistinguishable from Method 2. Values of R_p using Method 3 cannot be precisely reproduced.
- (4) In calculating polarization resistance (corrosion rates) either Methods 2 or 3 can be used.

=====
RBR, 24Aug04

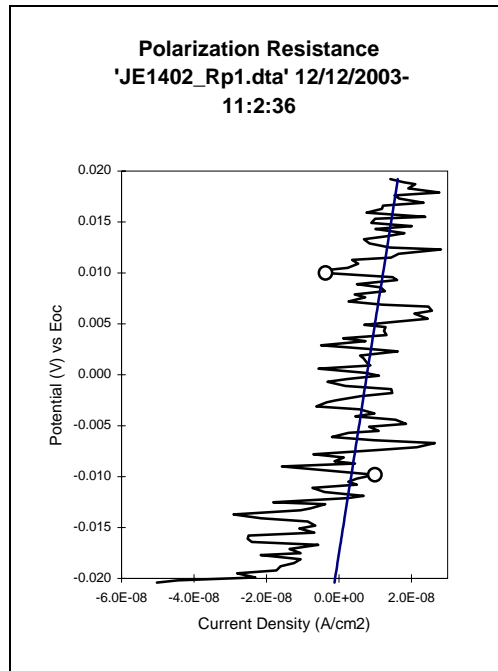


Figure 1a: Polarization Resistance calculated according to Launcher 3.10.
 $R_p = 2.27 \times 10^6 \text{ Ohm.cm}^2$

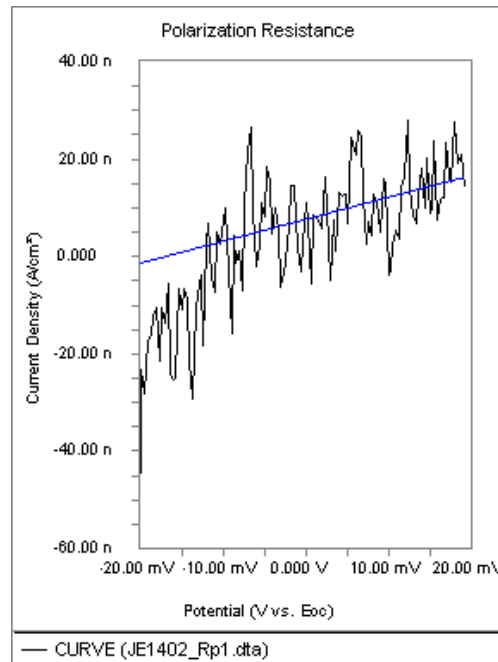


Figure 1b: Polarization Resistance calculated according to Echem Analyst 1.3 by reversing the axes (Method 2). $R_p = 2.27 \times 10^6 \text{ Ohm.cm}^2$

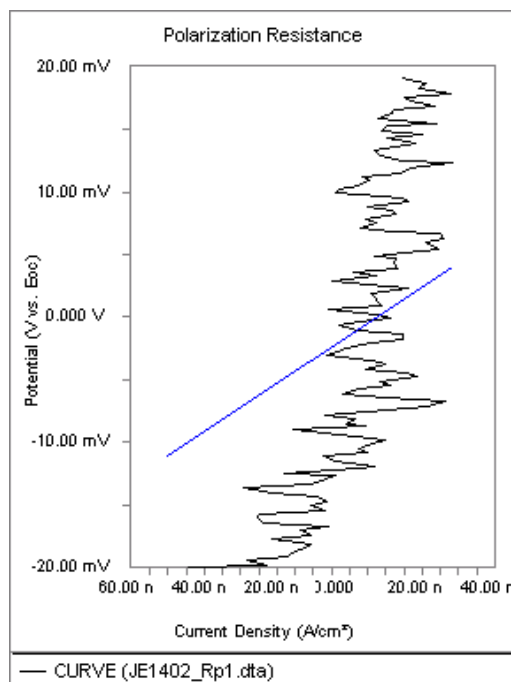


Figure 2: Polarization Resistance calculated according to Echem Analyst 1.3 when potential appears in X and current in Y (Method 1). $R_p = 1.925 \times 10^5 \text{ Ohm.cm}^2$

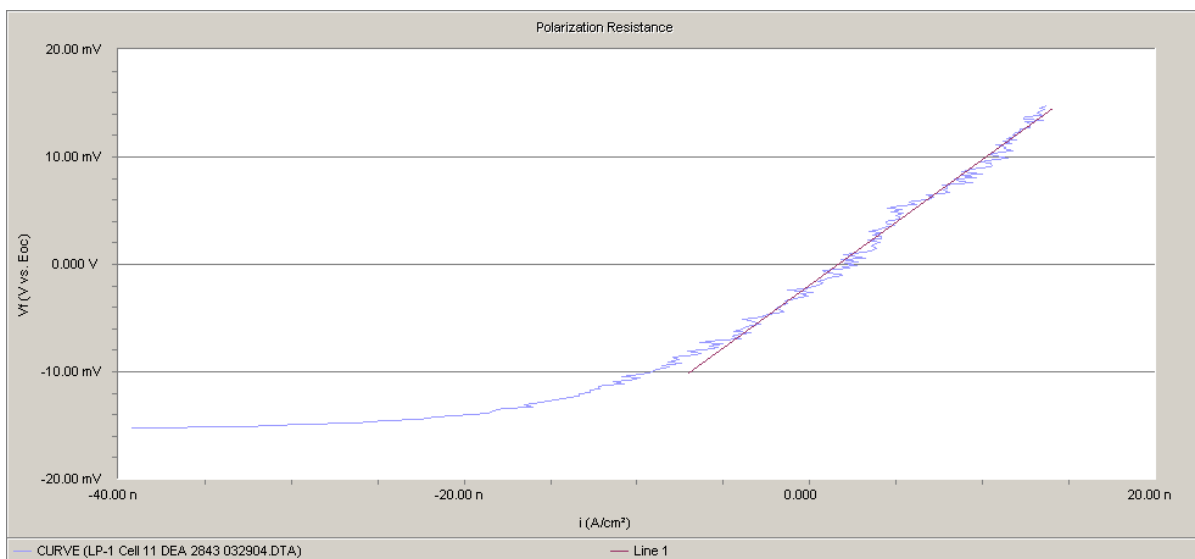


Figure 3: Polarization Resistance calculated according to Echem Analyst 1.3, Method 3 (Manual Fitting), Potential in Y and Current in X. Specimen DEA2843 immersed in 0.1 M Oxalic Acid at 30°C for 757 days (Measured on 29Mar04), $R_{p1} = 1.171 \times 10^6 \text{ Ohm.cm}^2$

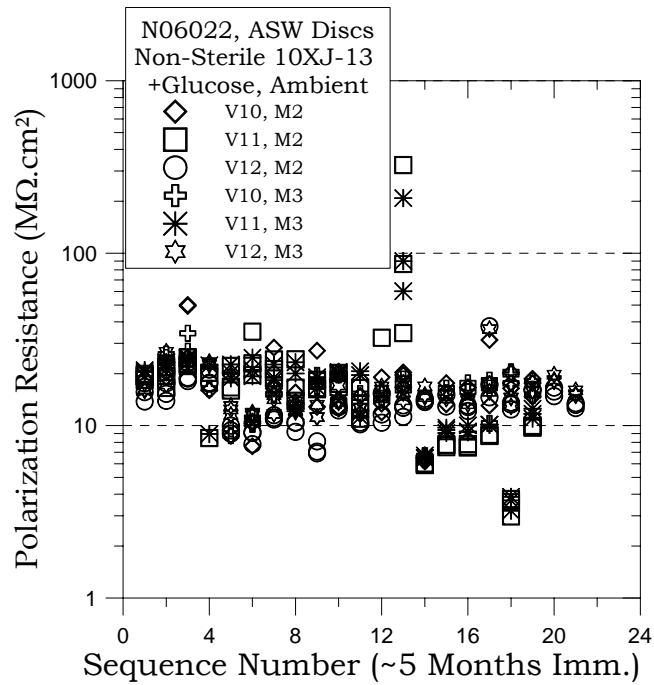


Figure 4: Polarization Resistance in Non-Sterile Environment using Methods 2 and 3.

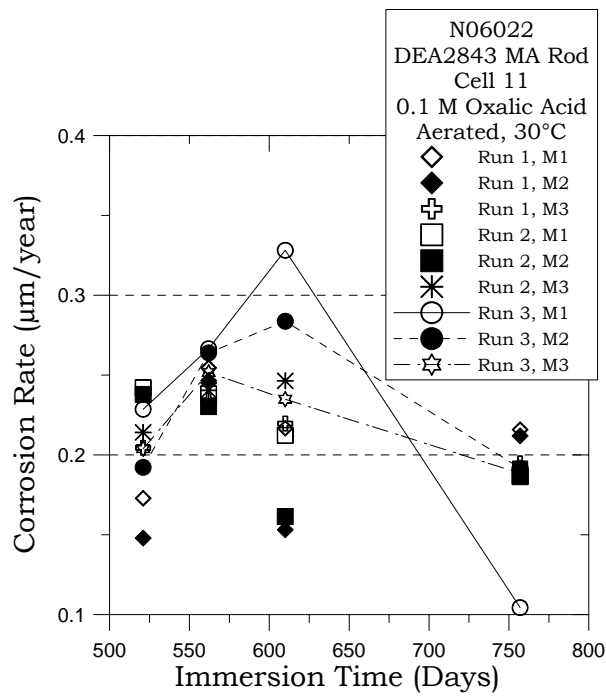


Figure 5: Corrosion Rate of Alloy 22 in oxalic acid using the 3 Methods.

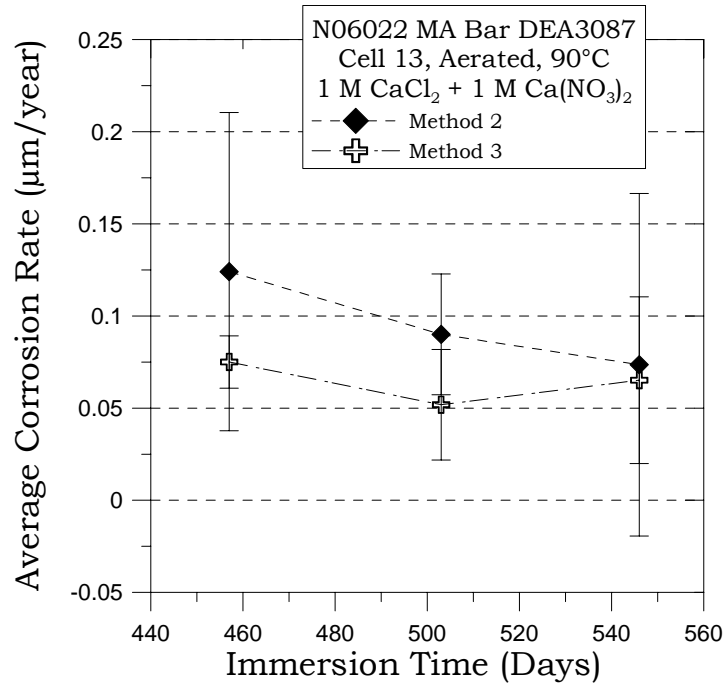


Figure 6: Corrosion Rates of Alloy 22 in 1 M CaCl₂ + 1 M Ca(NO₃)₂ at 90°C.

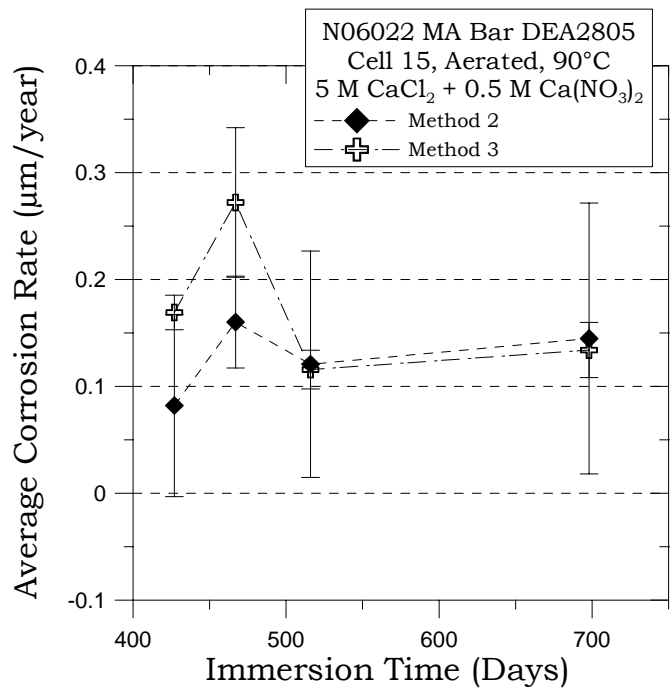


Figure 7: Corrosion Rates of Alloy 22 in 0.5 M CaCl₂ + 0.5 M Ca(NO₃)₂ at 90°C (Cell 15).

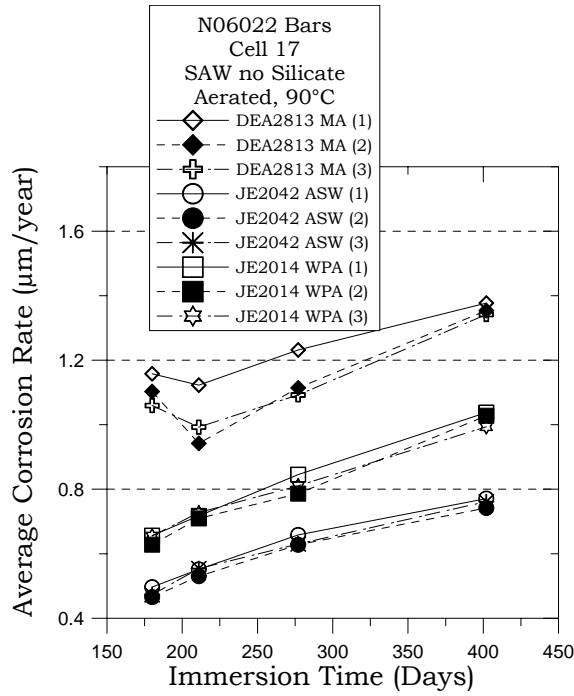


Figure 8: Corrosion Rates of Alloy 22 in SAW No-Silicate, 90°C (Cell 17).

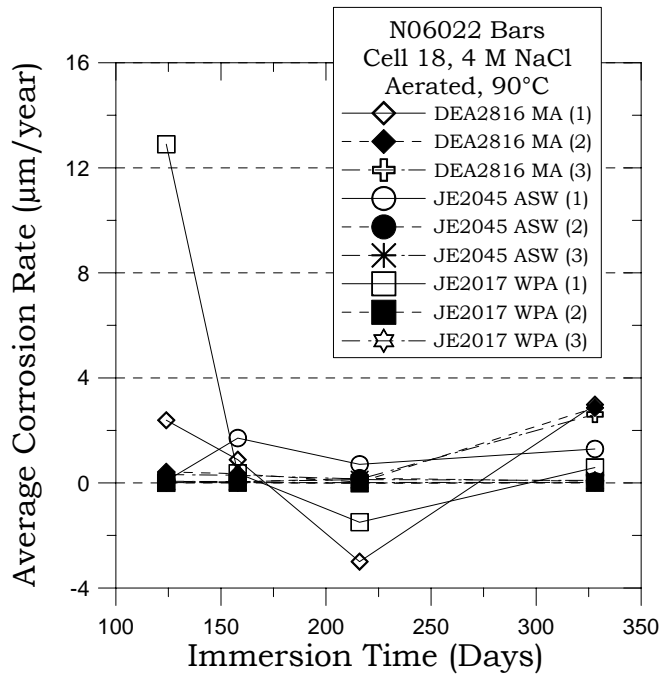


Figure 8: Corrosion Rate of Alloy 22 in 4 M NaCl at 90°C (Cell 18).

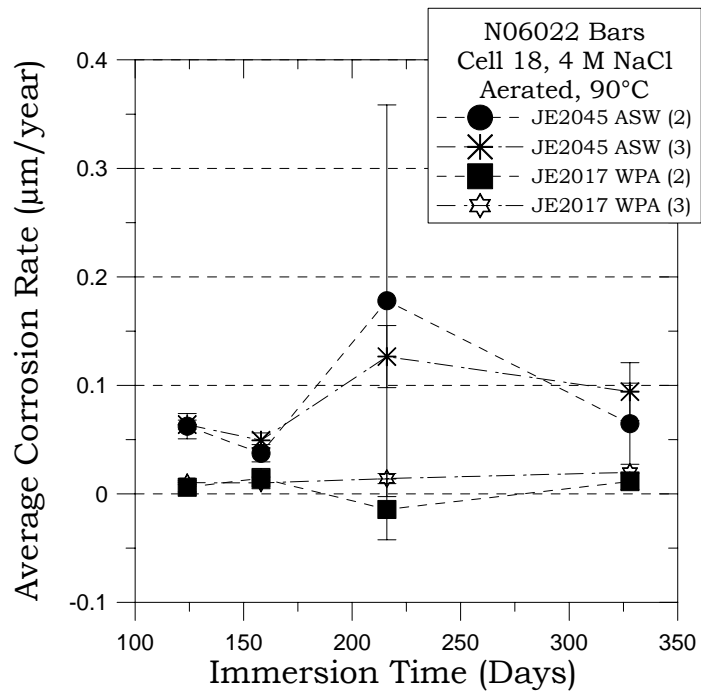


Figure 88 Corrosion Rate of Alloy 22 in 4 M NaCl at 90°C (Cell 18) using Methods 2 and 3 for ASW and WPA specimens only.

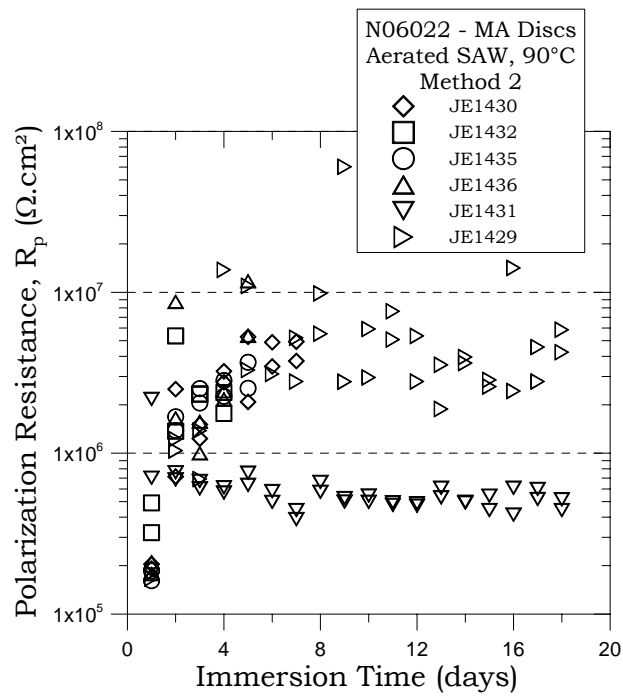


Figure 11: Polarization Resistance of Alloy 22 in aerated SAW at 90°C (Method 2).

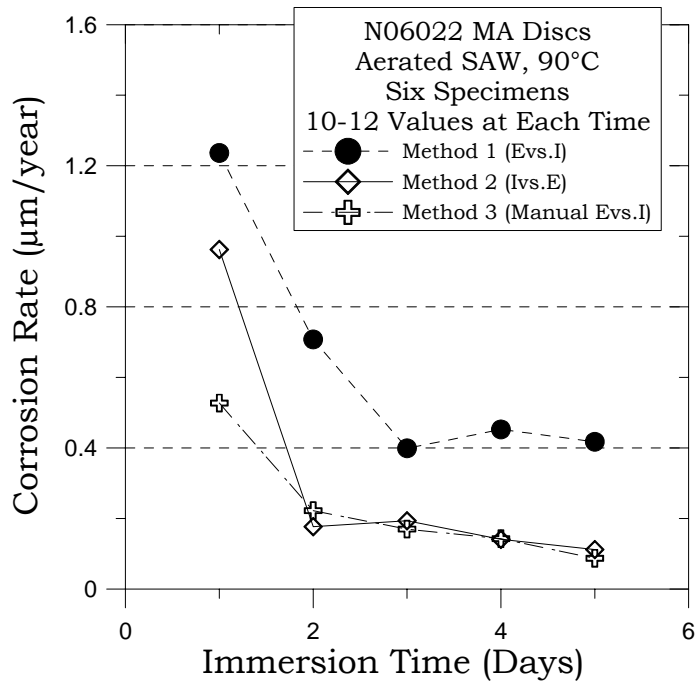


Figure 12: Average Corrosion Rates of Alloy 22 in aerated SAW at 90°C (Methods 1-3).

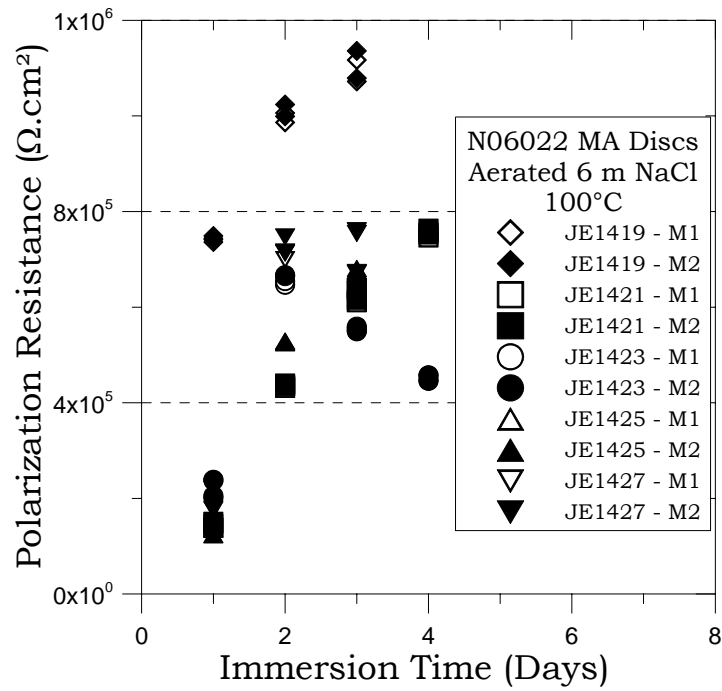


Figure 13: Polarization Resistance of Alloy 22 in aerated 6 m NaCl at 100°C.

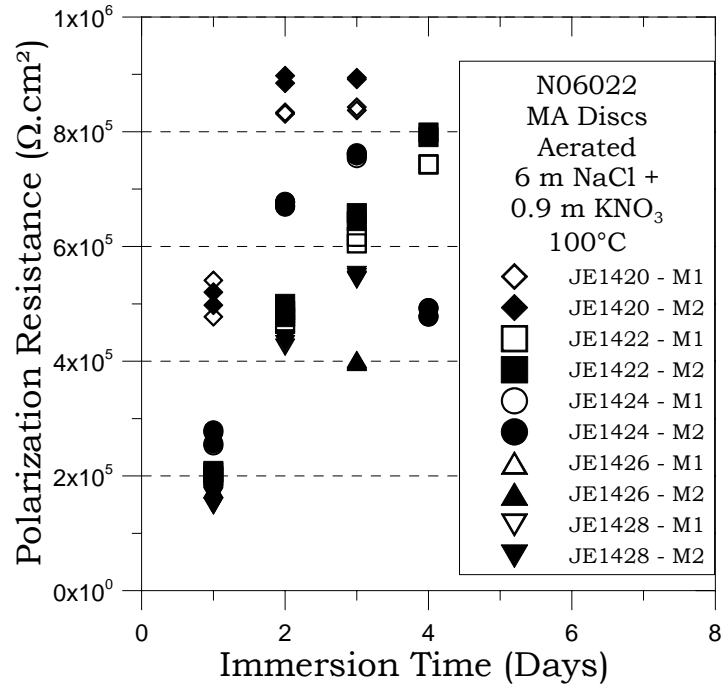


Figure 14: Polarization Resistance of Alloy 22 in aerated 6 m NaCl + 0.9 m KNO₃ at 100°C

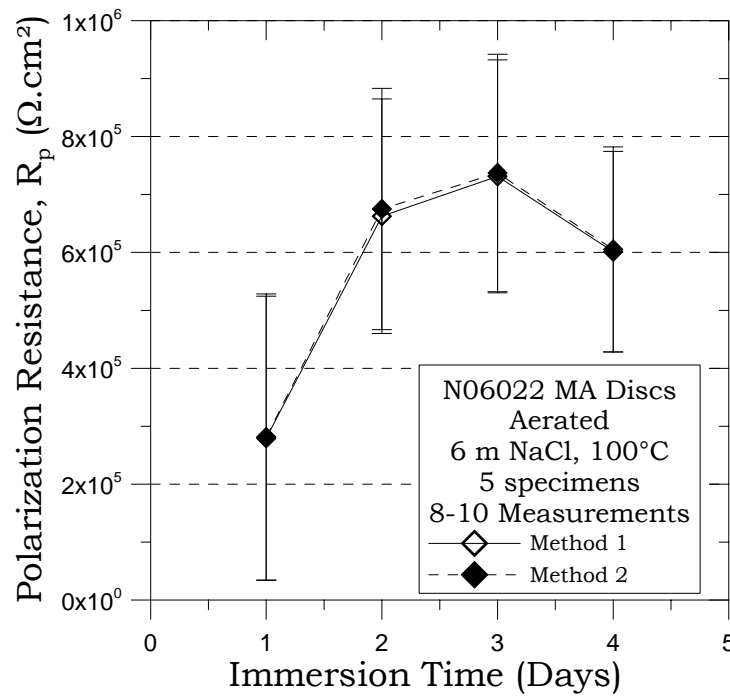


Figure 15: Average Polarization Resistance of Alloy 22 in aerated 6 m NaCl at 100°C.

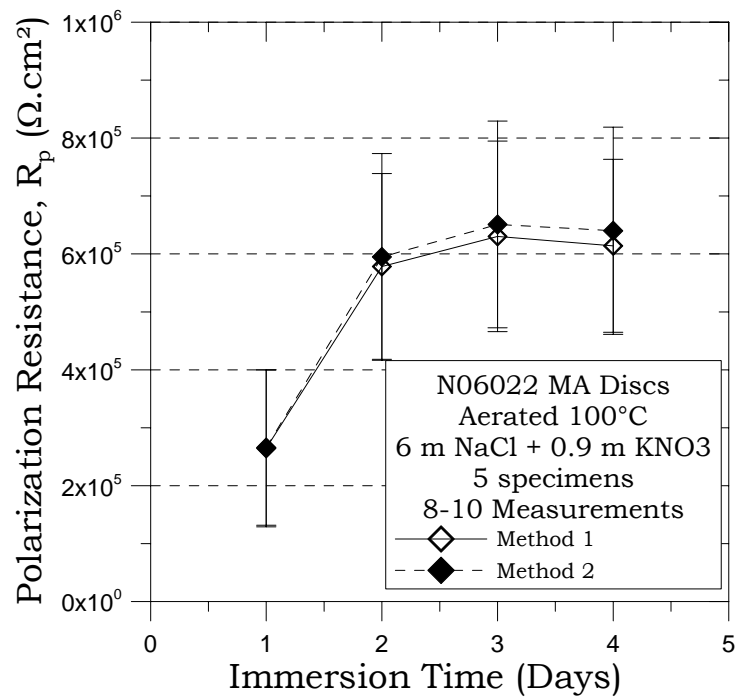


Figure 16: Average Polarization Resistance of Alloy 22 in aerated 6 m NaCl + 0.9 m KNO₃ at 100°C